IET Computer Vision

Special Issue: Computer Vision in Cancer Data Analysis

IET Journals
The Institution of Engineering and Technology

Automated skin lesion segmentation of dermoscopic images using GrabCut and k-means algorithms

ISSN 1751-9632
Received on 29th December 2017
Revised 9th June 2018
Accepted on 12th June 2018
E-First on 30th July 2018
doi: 10.1049/iet-cvi.2018.5289
www.ietdl.org

Seetharani Murugaiyan Jaisakthi[1], Palaniappan Mirunalini[2] ✉, Chandrabose Aravindan[2]

[1]*School of Computer Science and Engineering, Vellore Institute of Technology, Vellore, India*
[2]*Department of Computer Science and Engineering, SSN College of Engineering, Chennai, India*
✉ *E-mail: miruna@ssn.edu.in*

Abstract: Skin cancer is the most common type of cancer in the world and the incidents of skin cancer have been rising over the past decade. Even with a dermoscopic imaging system, which magnifies the lesion region, detecting and classifying skin lesions by visual examination is laborious due to the complex structures of the lesions. This necessitates the need for an automated skin lesion diagnosis system to enhance the diagnostic capability of dermatologists. In this study, the authors propose an automatic skin lesion segmentation method which can be used as a preliminary step for lesion classification. The proposed method comprises two major steps, namely preprocessing and segmentation. In the preprocessing step, noise such as illumination, hair and rulers are removed using filtering techniques and in the segmentation phase, skin lesions are segmented using the GrabCut segmentation algorithm. The k-means clustering algorithm is then used along with the colour features learnt from the training images to improve the boundaries of the segments. To evaluate the authors' proposed method, they have used ISIC 2017 challenge dataset and PH^2 dataset. They have obtained Dice coefficient values of 0.8236 and 0.9139 for ISIC 2017 test dataset and PH^2 dataset, respectively.

1 Introduction

One of the biggest threats to human beings is cancer and it is the second leading cause of death. Of all the cancer types, skin cancer is the most common form which is rapidly increasing in the recent years. Skin cancer is the uncontrolled growth of abnormal skin cells. These cancer cells may spread from the skin into other tissues and organs if left unchecked. Dermoscopy is a non-invasive imaging method used to detect melanoma and other skin lesions. With the help of dermoscopy, subsurface structures of skin lesions can be analysed and different types of lesions can be distinguished with better visualisation. The most common types of skin cancer [1–3] are

- *Basal cell carcinoma (BCC):* BCC is the most common form of skin cancer. Generally, it begins to grow from the bottom of the outer skin layer and develops in the area that is exposed to sunlight for long term. BCC is slow in growth and hence can be treated very easily. BCC appears as small, smooth, shiny, pale or waxy lump which may be red or brown in colour with rough, dry or scaly patches.
- *Squamous cell carcinoma (SCC):* SCC is the second most common type of cancer. The development of SCC starts in the outer skin layer and infiltrates the underlying tissues if left unchecked. This cancer spreads to other parts of the body and at its early stage, SCC can be easily treated. SCC also appears as small shinny lumps with red or brown in colour.
- *Malignant melanoma (MM):* Melanoma is more dangerous but less common type of skin cancer. It occurs in the melanocytes (cells that produce pigment) and it is the leading cause of skin cancer mortality. Melanoma is asymmetric in shape with an irregular border and uneven in colour.

Among all the cancer types, melanoma is the most dangerous form of skin cancer which leads to the highest degree of the death rate. Melanoma has a very high tendency to grow and even after removing the lesions may sometimes grow back. It may intrude and damage nearby organs and tissues and may invade other parts of the body where it is very hard to treat.

Generally, skin cancer is screened by clinicians through visual examination. During the screening of cancer, the clinicians look for moles and other spots that are different in colour from the normal skin. Visual screening by dermatologists for skin cancer does not guarantee 100% detection and sometimes it may lead to potential harm. Potential harm includes unnecessary procedures such as skin biopsy for lesions that do not turn out to be cancer or sometimes the lesions might have been missed and not have gone for biopsy, resulting in death. From the literature, it has been shown that even for experienced dermatologist the diagnostic accuracy rate is 60% [4–6] with a visual examination. As a result, there is a clear requirement for automatic detection systems for skin cancer which should be highly accurate and help in the overall analysis of a skin lesion.

The basic approach in developing an automatic diagnostic tool for skin lesion analysis includes segmentation, feature extraction and classification. Among these three tasks, segmentation is important since the accuracy of segmentation directly affects successive tasks. However, segmentation of a lesion is very hard because lesion shape, size, boundaries and colour vary greatly with the difference in the type of skin and texture. Apart from these variations, the lesion boundaries are also irregular and the transition from the lesion to skin is very smooth making the discrimination of normal skin and lesion very complex. Moreover, dermoscopic images include various artefacts such as air bubbles, hair, ink markings and so on, making the segmentation process challenging.

Recently, many methods for automatic segmentation and classification of skin lesions from dermoscopic images have been proposed to address these issues. The methods used for segmentation of the lesion can be widely classified as region-based, edge-based and threshold-based segmentation algorithms [7, 8].

A saliency-based lesion segmentation framework for segmenting lesion regions from dermoscopic images was proposed in [9]. The proposed approach separates the background by analysing the image region, boundaries and colour characteristics of dermoscopic images. Lesions are then localised by constructing a Bayesian framework using reconstruction error estimated by comparing the similarities of pixels in the lesion region and

background. Segmentation of lesions in dermoscopic images using a fixed-grid wavelet network (FGWN) was proposed by Sadri *et al.* [10]. The proposed FGWN takes R, G, B values of the dermoscopic image as input and use orthogonal least squares algorithm to estimate network weights and optimise the network structure. The output of the network describes the boundary of the skin lesion region. A new data model for the graph-cut method was proposed in [11] which takes the colour feature, texture and shape information for segmentation. The method automatically derives a seed pixel to train the classifier from a coarse initial segmentation of the pigmented skin lesions obtained by clustering and morphological operators.

In [12] a region-based active contour method was applied to extract the lesion border and was tested with 320 dermoscopic images. Skin lesion segmentation using Delaunay triangulation (DT) was proposed by Pennisi *et al.* [13]. The authors have used the publicly available PH^2 dataset to test the proposed method. Ma and Tavares [14] proposed an approach to segment skin lesions in dermoscopic images using a deformable model. The method uses the difference in illumination and saturation of skin lesion and normal healthy skin as a segmentation clue to segment lesion regions. Abbas *et al.* [15] used least-squares method and dynamic programming method to find the optimal boundary of the lesions. Silveira *et al.* [8] proposed and evaluated six different segmentation methods based on thresholding, edge-based and region-based algorithms using 100 dermoscopic images of melanocytic lesions. An automated skin lesion segmentation method using image-wise supervised learning and multi-scale superpixel-based cellular automata (CA) was proposed in [16].

An automatic border detection method based on colour space analysis and histogram thresholding was proposed by Garnavi *et al.* [17]. In this method, the lesion border was identified by first determining the optimal colour channel followed by hybrid thresholding and morphological operators. Gomez *et al.* [18] proposed an independent histogram pursuit which calculates a set of linear combinations of image bands to enhance the structures in the lesion images. Lesions are localized from these enhanced images using histogram thresholding. Yuksel and Borlu [19] proposed type-2 fuzzy logic techniques for an automatic threshold determination that is used to segment pigmented skin lesion images from dermoscopic images. An automatic segmentation method was proposed in [20] which extracts lesion borders using saliency map constructed with the help of colour and brightness and combined with Ostu threshold. A new mean shift-based fuzzy c-means algorithm was proposed in [21]. The method effectively segments clusters within the image, by finding reliable cluster centres by incorporating the mean field term within the standard fuzzy c-means as the objective function. A method to improve accuracy and to remove redundant computation in fast density-based lesion detection in dermoscopy images for the improved border was proposed in [22]. Fengying and Alan [23] have proposed a segmentation algorithm for dermoscopy images using self-generating neural networks seeded by genetic algorithm to obtain optimised and stabilised clustering. A machine learning approach was proposed in [24] to quantify significant colours in dermoscopy images. A fast and unsupervised approach for border detection in dermoscopy images was proposed using statistical region merging algorithm in [25].

Celebi *et al.* [7] briefly summarise the techniques and methods for artefact removal and contrast enhancement. They also provided a summary of 18 algorithms with their characteristics and reported performance evaluation, issues and proposed guidelines for automated border detection. A comparative study of several hair removal methods such as linear interpolation, inpainting by PDE non-linear diffusion and exemplar-based methods were presented in [26]. They also proposed a hair segmentation and repair algorithm using fast marching image inpainting technique. The hair and ruler marking was segmented using a canny edge detector and it has been refined further using morphological operators was proposed in [27].

Recently, many approaches for segmenting skin lesions using deep learning technique have been proposed. Bozorgtabar *et al.* [28] proposed a fusion method to segment skin lesions in dermoscopic images. In this work, the authors used fully convolutional network (FCN) to segment the global map of the lesion and super pixel technique to obtain the local lesion map. The obtained global and local maps are then combined to segment lesion region. A multistage segmentation approach using multiple FCNs was used to learn complementary visual characteristics produced at individual stages to achieve accurate localisation and well-defined lesion boundaries was proposed in [29].

An automated method to classify the segmented lesions was proposed in [30] using deeper networks and residual learning technique. The segmented input helps in extracting specific and representative features within the lesion regions for more accurate recognition of lesions. Extraction of the skin lesion region was obtained using the deep CNN, which combines local and global contextual information and outputs a segmentation mask which is further refined using a postprocessing technique [31].

Many preprocessing techniques for hair removal were also studied in the literature during the recent years. George *et al.* [32] proposed a preprocessing algorithm for skin hair and markers removal from 2D psoriasis skin images. The proposed hair removal method was based on contrast enhancement and morphological operations to detect the hair pixels and image interpolation was performed to replace hair pixels with neighbouring pixels through image inpainting method. The removal of markers was based on Ostu's thresholding and shape features. Maglogiannis and Delibasis [33] proposed different hair removal methods and compared the performance of the methods using original and synthetic hair.

In this paper, we propose an automatic system for segmenting skin lesions in the dermoscopic images which can be used as a preliminary step for skin lesion classification. This system identifies and locates lesion regions automatically and reduces the burden of a dermatologist in skin cancer diagnosis. The proposed method consists of two major steps. (i) Preprocessing, which removes the artefacts such as hair, ink markings, ruler images and illumination defects. (ii) Segmentation of lesions using GrabCut, k-means clustering and colour histogram features. To evaluate the performance of the proposed method we have used ISIC 2017 dataset [34] and PH^2 dataset [35] and obtained Dice coefficient values of 0.8236 and 0.9139, respectively, for the two datasets.

The remaining of the paper is organised as follows. Section 2 presents the general framework and details of the proposed methodology to segment skin lesions. In Section 3, the results of the proposed method and comparative discussion of the results are reported. Finally, concluding remarks and possible future directions are presented in Section 4.

2 Proposed methodology

We propose a semi-supervised learning technique to automatically segment skin lesion in a given image. The method includes two major steps namely preprocessing and segmentation. The preprocessing step is applied to filter out the artefacts present in an image and this filtered image is further used for segmenting the skin lesion. The segmentation is done with GrabCut and k-means clustering algorithms. The workflow of the proposed method is depicted in Fig. 1 and is explained in Algorithm 1.

Algorithm 1: Segmentation of lesion from a dermoscopic image
Input: Dermoscopic image D.
Output: Binary mask of the skin lesion M.

1: Downscale the image D using bi-linear interpolation and let the downscaled image be D' (Section 2.1.1).
2: Apply CLAHE algorithm to D' to obtain an illumination corrected image I (Section 2.1.2).
3: Apply Frangi 2D filter to enhance hairs in I as set of bright lines B (Section 2.1.3).
4: **for** each B_i in I **do**
5: Replace B_i with the background using FM inpainting algorithm
6: **end for**

7: Apply GrabCut segmentation algorithm to segment foreground F from I (Section 2.2.1).
8: Apply k-means clustering algorithm on F with $k = 4$ (Section 2.2.2).
9: Filter out interior clusters C_i using colour histogram (Section 2.2.2).
10: Extract the boundary region of filtered clusters using flood-fill algorithm (Section 2.2.3).
11: Merge the interior and boundary region to obtain a segmented skin lesion.
12: Create a binary mask M of the segmented lesion and upscale it using bi-linear interpolation method to the size of the original image (Section 2.2.4).

2.1 Preprocessing

The structure of skin lesions in dermoscopic images greatly varies based on the skin condition. The artefacts such as hair, air bubbles, gel ink marks, ruler images and contrast variations make the segmentation process difficult. So, to improve the accuracy of the lesion segmentation, we have applied the following preprocessing techniques.

2.1.1 Image scaling: The resolution of the dermoscopic images is usually very high. So, to reduce the computational complexity, the input images are scaled down to 25% using bi-linear interpolation method.

2.1.2 Illumination correction: Illumination correction technique is applied to remove uneven illumination of the image caused by sensor faults. The downscaled image is first converted into Lab colour space and then contrast limited adaptive histogram equalisation (CLAHE) algorithm [36, 37] is applied to L channel. CLAHE is the upgraded version of adaptive histogram equalisation (AHE) which overrides the drawback of standard histogram equalisation. In CLAHE, the image is split up into small blocks called tiles. Histogram equalisation is applied to each of these tiles. To avoid amplification of noise in the image, contrast limiting is applied. Contrast limiting clips and distributes the pixels which are above the contrast limit uniformly to other bins before applying histogram equalisation. Finally, the neighbouring tiles are merged using bilinear interpolation to remove artefacts in the boundaries. The contrast enhanced L channel is then merged to form a Lab image and then converted into an RGB image.

2.1.3 Hair removal: Dermoscopic images often contain hairs which make the segmentation process hard because the hair pixels occlude important features such as boundary and texture. The presence of hair also makes the feature extraction process more difficult. In the proposed method, Frangi vesselness algorithm [38] along with fast march method (FMM) [39] have been used to remove the hairs in the image.

Once the hair regions in the images are identified using Frangi vesselness filter, an inpainting technique using FMM is used to replace the hair pixels. FMM inpaints the hair region by propagating an image smoothness estimator starts from the boundary region and goes inside the region gradually, filling every pixel. The image smoothness is calculated as the weighted average over a small known neighbourhood around the pixels to inpaint. The algorithm keeps moving to the next nearest pixel using FMM once a hair pixel is inpainted. We have chosen FMM algorithm since it is an efficient inpainting algorithm, faster than other inpainting methods and it clearly specifies which is the next pixel to inpaint by explicitly maintaining a narrow boundary between the source image and vessel enhanced image. Figs. 2*a* and *b* show the result of applying the preprocessing techniques for sample images from ISIC 2017 and PH^2 datasets.

2.2 Segmentation

Segmentation is the process of isolating the diseased area from normal skin based on the homogeneity of the pixels. Homogeneity of the pixels may be determined by colour and texture features. We have used colour features of the diseased area in order to partition the skin lesion regions.

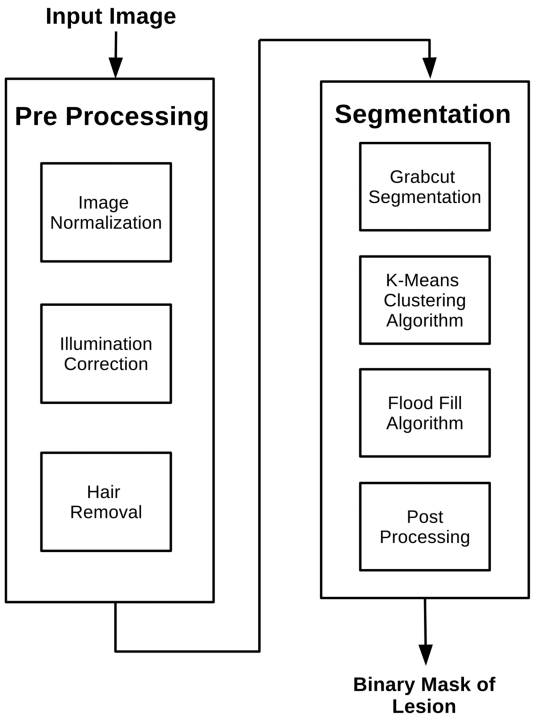

Fig. 1 *Block diagram of the proposed skin lesion segmentation*

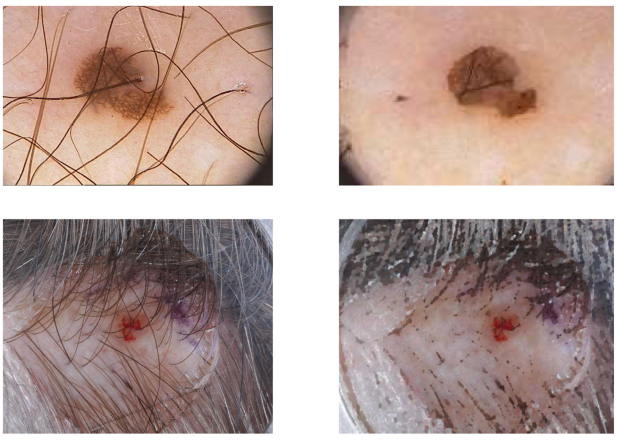

Fig. 2 *Results of applying preprocessing techniques for sample images* ***(a)*** Input Image, ***(b)*** Preprocessed Image

The proposed skin lesion segmentation method consists of two major phases. During the first phase, the GrabCut segmentation algorithm is applied to localise the approximate lesion region and then clustering algorithm is applied to the segmented image to localise exact lesion region. The detailed description of these phases is discussed in the following section.

2.2.1 GrabCut segmentation: The skin lesion images do not have defined edges and the region is highly irregular in shape making the segmentation process challenging. Most of the segmentation algorithms make use of either edge or region information for segmenting the objects in the images. However, the GrabCut segmentation algorithm utilises both the boundary and region information in order to segment the foreground image. So, to locate the global lesion region in a dermoscopic image, we have applied the GrabCut segmentation algorithm. The located region is then fine-tuned to the segment lesion region using a k-means clustering algorithm.

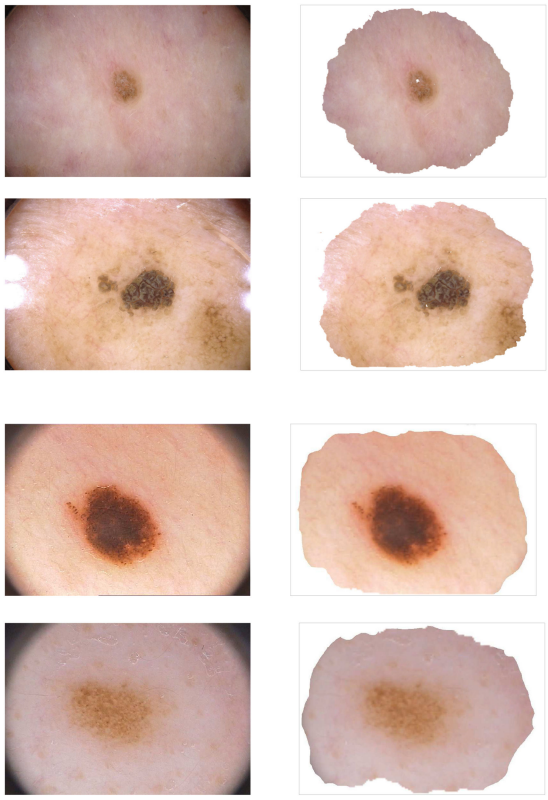

Fig. 3 *Results of GrabCut segmentation for the sample images from ISIC 2017 validation set and* PH^2 *dataset*
(a) Input Image, ***(b)*** Segmented foreground image

The GrabCut segmentation algorithm takes two inputs T_B, a set of background pixels and T_F a set of foreground pixels. Initial T_B and T_F are chosen automatically by drawing a rectangle around the object of interest where every pixel outside this rectangle is considered as a background pixel and every pixel inside the rectangle is considered as a foreground pixel. The rectangle is drawn automatically by choosing $(0.1 \times w, 0.1 \times h)$ as a top left corner and $(0.9 \times w, 0.9 \times h)$ as a bottom right corner, where w and h are width and height of the image, respectively. In some of the dermoscopic images, the lesion region may extend to one of the corners or edges. In these cases, the GrabCut algorithm may consider some part of the lesion region as background.

Based on the given input, the algorithm first labels the foreground and background pixels and two Gaussian mixture models (GMMs), each having five Gaussians, are developed, one for the foreground and the other for the background. GrabCut then builds a weighted directed graph where the pixels in the images are regarded as nodes. Two more additional nodes namely source node and sink node are added to the graph. The pixels in the foreground are connected to the source node and similarly, pixels in the background are connected to the sink node. Weights (D) for the edges between pixel and source or sink node are assigned based on the probability of a pixel being foreground or background. The cost of assigning the individual pixel to the foreground or the background is represented by the edges.

Given $\boldsymbol{z}_n$ the vector of pixels from RGB colour space, $\boldsymbol{\alpha}_n$ the result of segmentation which is given by vector of labels (0 stands for the background and 1 stands for the foreground), θ histograms showing pixel value distribution of foreground and background labels and $\boldsymbol{k}_n$ additional vector assigning to each pixel a unique GMM component (either from the background or from the foreground, based on $\alpha = 0$ or 1), the data term U for colour GMM model is defined by

$$U(\alpha, k, \theta, z) = \sum_n D(\boldsymbol{\alpha}_n, \boldsymbol{k}_n, \theta, \boldsymbol{z}_n) \tag{1}$$

where

$$D(\boldsymbol{\alpha}_n, \boldsymbol{k}_n, \theta, \boldsymbol{z}_n) = -\log p(\boldsymbol{z}_n | \boldsymbol{\alpha}_n, \boldsymbol{k}_n, \theta) - \log \pi(\boldsymbol{\alpha}_n, \boldsymbol{k}_n) \tag{2}$$

where $p(.)$ represents a Gaussian probability distribution and $\pi(.)$ are mixture weighting coefficients. Therefore, the parameters of the model are

$$\theta = \pi(\alpha, k), \mu(\alpha, k), \Sigma(\alpha, k), \quad \alpha = (0, 1), k = (1, \ldots, K) \tag{3}$$

The weights for the edges between the pixels are assigned based on the pixel colour similarity. If the difference in pixel colour is very large then the edge (V) between those pixels will get low weight/cost. The smoothness term V is given by

$$V(\alpha, z) = \gamma \sum_{(m,n) \in C} \text{dis}(m, n)^{-1} [\alpha_n \neq \alpha_m] e^{-\beta \| z_m - z_n \|^2} \tag{4}$$

where C defines the set of pairs of neighbouring pixels, γ and β are constants whose values are taken from [40] and dis(.) is the Euclidean distance of neighbouring pixels.

The mincut algorithm is then used to cut the graph into two distinct source node and sink node with minimum cost function (E). After the cut, the pixels that are connected to the source node are marked as foreground and those that are connected to the sink node are marked as background. The entire process is repeated until the classification converges or for a fixed number of iterations

$$E(\alpha, k, \theta, z) = U(\alpha, k, \theta, z) + V(\alpha, z) \tag{5}$$

The result of applying GrabCut segmentation for samples images from ISIC 2017 validation set is depicted in Figs. 3*a* and *b*. GrabCut algorithm locates the approximate lesion region by eliminating some of the background information. The segmented region contains the lesion region as well as some part of background information. In order to extract the exact lesion region with improved boundaries, the segmented foreground image is further processed using clustering techniques.

2.2.2 k-means clustering: The segmented foreground image obtained from the GrabCut algorithm is further processed using the k-means clustering algorithm [41, 42]. We have used the k-means clustering algorithm to group the pixels of the obtained foreground image in RGB colour space. The cluster centres are chosen in such a way that cluster centres are far apart to reduce the probability of bad initialisation as proposed by Arthur and Vassilvitskii [43]. The method picks first cluster centre randomly from the input pixels. Each subsequent cluster centre is identified from the rest of the pixels, based on the probability proportional to its squared distance from the pixels' closest existing cluster centre. The input pixels are grouped into

i. interior skin lesion,
ii. lesion boundary,
iii. lesion background (normal skin),
iv. background image.

From the obtained clusters, the cluster with pixel colour which is similar to skin lesion colour is retained. To identify the cluster to be retained as a lesion, our method automatically learns the pixel colour information from the training images by constructing colour histograms. From the constructed histogram the upper and lower boundaries of the pixel intensities are obtained. The cluster with a pixel intensity that lies within the estimated threshold values is filtered out. From the remaining clusters, the lesion boundary region is identified using the flood-fill algorithm described in the following steps. The result of applying k-means clustering algorithm for sample images in ISIC 2017 validation set and PH^2 dataset is shown in Fig. 4.

2.2.3 Segmentation using flood fill: The output of the k-means is the core of the lesion region and the boundary part may be missing.

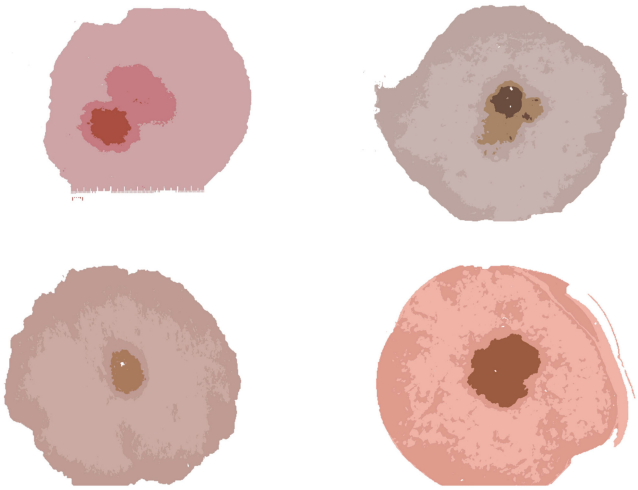

Fig. 4 *Results of k-means clustering for sample images in ISIC 2017 validation set*

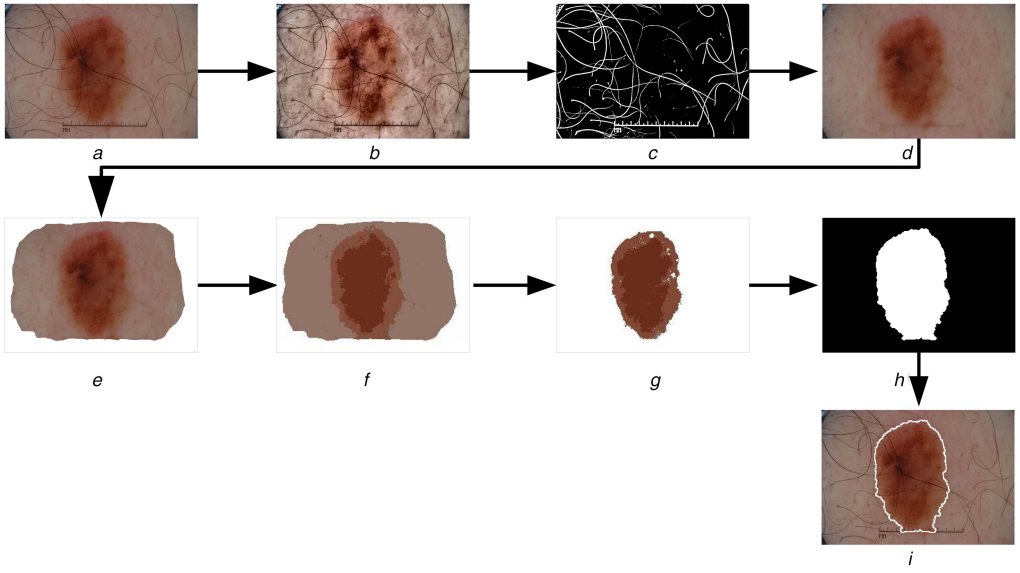

Fig. 5 *Steps involved in segmenting skin lesion region using the proposed method*
(a) Input image, ***(b)*** Illumination corrected image, ***(c)*** Vesselness (hair) enhanced image, ***(d)*** Hair inpainted image, ***(e)*** Foreground extracted image using grabcut, ***(f)*** Clusters formed using k-means, ***(g)*** Segmentation after flood fill, ***(h)*** Segmented binary mask, ***(i)*** Segmented lesion region overlapped with original image

To segment the lesion region with improved boundaries, a flood-fill algorithm is used. The flood-fill algorithm requires a seed point to fill the connected components which are of similar colour. This seed pixel is selected automatically by randomly choosing a pixel which is just beyond the boundary (within ten pixels) of the lesion cluster.

2.2.4 Postprocessing: The regions obtained using k-means clustering and flood-fill algorithms are combined and final lesion region is extracted by applying connected component labelling. The obtained region may contain holes and these holes are filled by applying a hole filling algorithm. The obtained image is converted into the binary mask and upscaled to the original size of the input image.

3 Results and discussion

3.1 Datasets

To evaluate the performance of the proposed system we have used ISIC 2017 [34] dataset and PH^2 [35] dataset. The first dataset was obtained from the ISIC 2017: Skin Lesion Analysis Towards Melanoma Detection challenge. The training images include 2000 dermoscopic lesion images in JPEG format paired with ground truth information. The ground truth file for each image is the binary mask image with a black pixel representing background and white pixel representing lesion region. The dataset also includes optional validation set with 150 images and test set with 600 images. The images in the dataset include three categories of cancer, namely Melanoma, Seborrheic Keratosis and Benign Nevi.

PH^2 dataset consists of 200 dermoscopic images of melanocytic lesions which includes 80 common Nevi, 80 atypical Nevi and 40 Melanomas. All the images are colour images with a resolution of 768×560 pixels. The ground truth for segmentation is also included in the dataset as binary masks.

3.2 Implementation

The proposed method was implemented using C & OpenCV. During preprocessing a probablity threshold of 0.5 was used to identify the hair region using Frangi Vesselness filter. The GrabCut segmentation algorithm was executed for ten iterations and k-means clustering algorithm was executed for seven iterations. Histograms were built using ISIC 2017 training dataset to learn the threshold ranges. Three different ranges were learnt corresponding to the three classes in the ISIC dataset. Since the number of iterations was fixed in Grabcut and k-means algorithms the overall complexity to process an image is $O(w \times h)$, where w and h are width and height of an image, respectively. Figs. 5*a–i* depict the steps involved in localising skin lesion region using the proposed technique for a sample image from the ISIC 2017 test set.

Figs. 6*a–c* show the results of our proposed method for sample images from ISIC 2017 and PH^2 datasets.

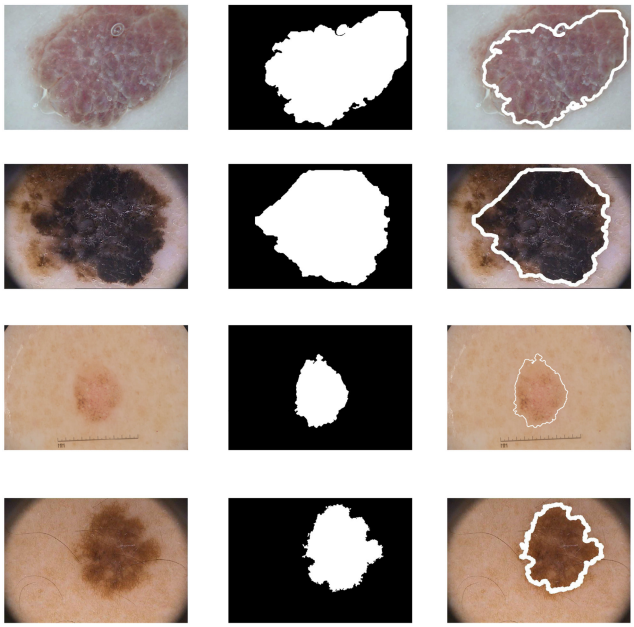

Fig. 6 *Results of the proposed method for sample images*
(a) Input image, ***(b)*** Segmented binary mask, ***(c)*** Segmented lesion region overlapped with the original image

Table 1 Results of the proposed method using ISIC 2017 dataset with and without preprocessing

	With preprocessing		Without preprocessing	
	Test set	Validation set	Test set	Validation set
accuracy	0.9193	0.9410	0.8779	0.8504
Dice coefficient	0.8236	0.8442	0.7141	0.6344
Jaccard index	0.7165	0.7398	0.6048	0.5303
sensitivity	0.8048	0.8559	0.7568	0.7852
specificity	0.9848	0.9835	0.9613	0.9056

Table 2 Results of the proposed method using PH^2 dataset with and without preprocessing

Performance metric	With preprocessing	Without preprocessing
	Values	Values
accuracy	0.9604	0.8577
Dice coefficient	0.9139	0.7714
Jaccard index	0.8437	0.6691
sensitivity	0.8900	0.7834
specificity	0.9879	0.9191

3.3 Performance evaluation

The proposed technique is evaluated using performance indices, namely accuracy (AC), sensitivity (SE), specificity (SP), Dice coefficient (DI) and Jaccard index (JA). The performance indices used are pixel level estimations. The pixel-level accuracy of segmentation is the estimation of how many lesion pixels are correctly identified when compared to the ground truth image. Sensitivity measures the amount of actual lesion pixels that are predicted as lesion pixels, while specificity measures the amount of actual background pixels that are identified as background pixels. Jaccard index and Dice coefficient estimate the degree of overlapping of ground truth and segmented lesion region.

To evaluate the performance of our proposed method, we have conducted different experiments on ISIC 2017 and PH^2 datasets. With these two datasets, we have evaluated the performance with and without the preprocessing technique and for ISIC 2017 dataset we have calculated performance for both validation and test set. Table 1 shows the average performance metric obtained for validation and test sets using ISIC 2017 dataset with and without preprocessing.

The Jaccard index estimates how well the extracted lesion region overlaps with the lesion region of the ground truth images. The obtained average Jaccard index values are 0.7165 and 0.7398 for the test and validation sets, respectively, with preprocessing steps. Our method has produced lower Jaccard index value for the images when the lesion and skin are very similar. A good accuracy of 0.9410 and 0.9193 has been achieved for validation and test sets, respectively. It has been noticed that the average values of all evaluated performance metrics are higher for preprocessed images than that of the images without preprocessing.

Table 2 shows the results of the proposed method for PH^2 dataset. Average sensitivity using PH^2 dataset with preprocessing is 0.8900 and the lowest sensitivity value obtained is 0.5318. And this shows that our technique has identified at least some part of the lesion region in the images. Similarly, the average accuracy for this dataset is 0.9604.

Our proposed method produced high Jaccard index and Dice coefficient values for both the datasets when the preprocessing technique is applied. This shows that the preprocessing technique is important in achieving good segmentation result.

Table 3 Comparison of our proposed method using PH^2 dataset

Method	Dice coefficient	Jaccard index	Accuracy	Sensitivity	Specificity	HM	XOR
robust saliency-based skin lesion segmentation [9]	0.9105	—	—	—	—	0.1549	0.1645
saliency combined with Otsu threshold [20]	0.8935	—	0.9360	0.8703	—	—	—
CA [9, 16]	0.8889	—	—	—	—	0.1986	0.1827
DT [13]	—	—	0.8960	0. 8024	0.9722	—	—
adaptive threshold [8, 9]	0.8191	—	—	—	—	0.2861	0.3949
Chan-level set method [8, 9]	0.8482	—	—	—	—	0.2458	0.2893
our method	**0.9139**	**0.8437**	**0.9604**	**0.8900**	**0.9879**	**0.1474**	**0.18723**

3.4 Comparison

The performance of our method is compared with that of existing techniques presented in [8, 9, 13, 16, 20] using PH^2 dataset. We have compared our results using similarity measures and also using dissimilarity measures. Dissimilarity measure can be calculated using Hammoude distance (HM) and XOR measure where lower values indicate better results.

Table 3 presents the comparison of our method with other methods using PH^2 dataset. With this dataset, our proposed method achieved a Dice coefficient of 0.9139 which is higher when compared to all the other methods. The method proposed by Ahn *et al.* [9] produced a Dice coefficient which is very close to our method but it fails to segment lesion region which is very small and visually not well defined. Our method detects this kind of lesion regions but sometimes misses a small part of lesions when the lesion extends beyond the border. Fan *et al.* [20] proposed a work based on saliency map features of colour and brightness. It handles inhomogeneity but fails to handle the fuzzy borders thus achieved a Dice coefficient of 0.8935. The method proposed in [16] achieved a Dice coefficient of 0.8889 but this method is computationally intensive as it estimates image wise supervised learning approach to select seed pixel. Adaptive thresholding and level set method [8] also obtained good results but both the methods are affected due to low contrast and inhomogeneity in pixel intensity and so these methods produced a high dissimilarity measure. DT [13] has estimated only accuracy, sensitivity and specificity which is less when compared to our method.

4 Conclusion and future work

In this paper, we have presented an automated method to segment skin lesion regions using a semi-supervised learning technique. This system helps dermatologists to automatically locate lesion regions in dermoscopic images for further diagnosis. Our method comprises two major steps, namely preprocessing and segmentation. During preprocessing, artefacts such as air bubbles, hair and ink marks are filtered out. To correct the illumination we have used the CLAHE algorithm and hairs are removed using Frangi vesselness and inpainting algorithms.

From the filtered image, lesion regions are segmented using GrabCut and clustering algorithms. The GrabCut algorithm segments the foreground image (lesion region) and k-means clustering and flood-fill algorithms are applied to obtain the lesion region with improved boundaries. To ascertain the performance of the proposed algorithm we have tested our method with ISIC 2017 dataset and PH^2 dataset for both preprocessed and non-preprocessed images. For both the datasets, we have obtained good accuracy of 0.91935 and 0.96047, respectively. The Dice coefficient values of 0.8236 and 0.9139 for ISIC 2017 test dataset and PH^2 dataset were obtained. The HM and XOR values for PH^2 dataset are 0.1474 and 0.18723, respectively. Deep learning techniques may be tried in the future to further improve accuracy and Dice coefficient values.

5 Acknowledgments

The authors express their sincere thanks to the managements of Vellore Institute of Technology, Vellore, India, and SSN College of Engineering, Chennai, India, for funding the respective Research Labs where this research was carried out. One of the authors, S.M. Jaisakthi, would like to thank NVIDIA for providing a GPU grant in support of this research work.

6 References

[1] Chuang, T.-Y., Popescu, A., Su, W.D., *et al.*: 'Basal cell carcinoma: a population-based incidence study in Rochester, Minnesota', *J. Am. Acad. Dermatol.*, 1990, **22**, (3), pp. 413–417

[2] Sigurdsson, S., Philipsen, P.A., Hansen, L.K., *et al.*: 'Detection of skin cancer by classification of Raman spectra', *IEEE Trans. Biomed. Eng.*, 2004, **51**, (10), pp. 1784–1793

[3] Camacho, F., Gildea, J., Goldenberg, G., *et al.*: '*Managing skin cancer*' (Springer, Berlin, Heidelberg, 2010), pp. 17–35

[4] Fleming, M.G., Steger, C., Zhang, J., *et al.*: 'Techniques for a structural analysis of dermatoscopic imagery', *Comput. Med. Imaging Graph.*, 1998, **22**, (5), pp. 375–389

[5] Grin, C.M., Kopf, A.W., Welkovich, B., *et al.*: 'Accuracy in the clinical diagnosis of malignant melanoma', *Arch. Dermatol.*, 1990, **126**, (6), pp. 763–766

[6] Morton, C.A., Mackie, R.M.: 'Clinical accuracy of the diagnosis of cutaneous malignant melanoma', *Br. J. Dermatol.*, 1998, **138**, (2), pp. 283–287

[7] Celebi, M., Iyatomi, H., Schaefer, G., *et al.*: 'Lesion border detection in dermoscopy images', *Comput. Med. Imaging Graph.*, 2009, **33**, (2), pp. 148–153

[8] Silveira, M., Nascimento, J.C., Marques, J.S., *et al.*: 'Comparison of segmentation methods for melanoma diagnosis in dermoscopy images', *IEEE J. Sel. Top. Signal Process.*, 2009, **3**, (1), pp. 35–45

[9] Ahn, E., Kim, J., Bi, L., *et al.*: 'Saliency-based lesion segmentation via background detection in dermoscopic images', *IEEE J. Biomed. Health Inf.*, 2017, **21**, (6), pp. 1685–1693

[10] Sadri, A.R., Zekri, M., Sadri, S., *et al.*: 'Segmentation of dermoscopy images using wavelet networks', *IEEE Trans. Biomed. Eng.*, 2013, **60**, (4), pp. 1134–1141

[11] Kehichian, R., Gong, H., Revenu, M., *et al.*: 'New data model for graph-cut segmentation: application to automatic melanoma delineation'. 2014 IEEE Int. Conf. on Image Processing (ICIP), Paris, France, October 2014, pp. 892–896

[12] Abbas, Q., Fondon, I., Rashid, M.: 'Unsupervised skin lesions border detection via two-dimensional image analysis', *Comput. Methods Programs Biomed.*, 2011, **104**, (3), pp. e1–e15

[13] Pennisi, A., Bloisi, D.D., Nardi, D., *et al.*: 'Skin lesion image segmentation using Delaunay triangulation for melanoma detection', *Comput. Med. Imaging Graph.*, 2016, **52**, pp. 89–103

[14] Ma, Z., Tavares, J.M.R.S.: 'A novel approach to segment skin lesions in dermoscopic images based on a deformable model', *IEEE J. Biomed. Health Inf.*, 2016, **20**, (2), pp. 615–623

[15] Abbas, Q., Celebi, M.E., Fondon Garcia, I., *et al.*: 'Lesion border detection in dermoscopy images using dynamic programming', *Skin Res. Technol.*, 2011, **17**, (1), pp. 91–100

[16] Bi, L., Kim, J., Ahn, E., *et al.*: 'Automated skin lesion segmentation via image-wise supervised learning and multi-scale superpixel based cellular automata'. 2016 IEEE 13th Int. Symp. on Biomedical Imaging (ISBI), Prague, Czech Republic, April 2016, pp. 1059–1062

[17] Garnavi, R., Aldeen, M., Celebi, M.E., *et al.*: 'Border detection in dermoscopy images using hybrid thresholding on optimized color channels', *Comput. Med. Imaging Graph.*, 2011, **35**, (2), pp. 105–115

[18] Gomez, D.D., Butakoff, C., Ersboll, B.K., *et al.*: 'Independent histogram pursuit for segmentation of skin lesions', *IEEE Trans. Biomed. Eng.*, 2008, **55**, (1), pp. 157–161

[19] Yuksel, M.E., Borlu, M.: 'Accurate segmentation of dermoscopic images by image thresholding based on type-2 fuzzy logic', *IEEE Trans. Fuzzy Syst.*, 2009, **17**, (4), pp. 976–982

[20] Fan, H., Xie, F., Li, Y., *et al.*: 'Automatic segmentation of dermoscopy images using saliency combined with Otsu threshold', *Comput. Biol. Med.*, 2017, **85**, pp. 75–85

[21] Zhou, H., Schaefer, G., Sadka, A.H., *et al.*: 'Anisotropic mean shift based fuzzy c-means segmentation of dermoscopy images', *IEEE J. Sel. Top. Signal Process.*, 2009, **3**, (1), pp. 26–34

[22] Suer, S., Kockara, S., Mete, M.: 'An improved border detection in dermoscopy images for density based clustering', *BMC Bioinf.*, 2011, **12**, (10), p. S12

[23] Fengying, X., Alan, C.B.: 'Automatic segmentation of dermoscopy images using self-generating neural networks seeded by genetic algorithm', *Pattern Recognit.*, 2013, **46**, (3), pp. 1012–1019

[24] Celebi, M.E., Zornberg, A.: 'Automated quantification of clinically significant colors in dermoscopy images and its application to skin lesion classification', *IEEE Syst. J.*, 2014, **8**, (3), pp. 980–984
[25] Celebi, M., Kingravi, H., Iyatomi, H., *et al.*: 'Border detection in dermoscopy images using statistical region merging', *Skin Res. Technol.*, 2008, **14**, (3), pp. 347–353
[26] Abbas, Q., Celebi, M.E., Garca, I.F.: 'Hair removal methods: a comparative study for dermoscopy images', *Biomed. Signal Proc. Control*, 2011, **6**, (4), pp. 395–404
[27] Bahreyni, T.M.T., Reza, P.H., Hoda, Z., *et al.*: 'An effective hair removal algorithm for dermoscopy images', *Skin Res. Technol.*, 2013, **19**, (3), pp. 230–235
[28] Bozorgtabar, B., Sedai, S., Roy, P.K., *et al.*: 'Skin lesion segmentation using deep convolution networks guided by local unsupervised learning', *IBM J. Res. Dev.*, 2017, **61**, (4), pp. 6:1–6:8
[29] Bi, L., Kim, J., Ahn, E., *et al.*: 'Dermoscopic image segmentation via multistage fully convolutional networks', *IEEE Trans. Biomed. Eng.*, 2017, **64**, (9), pp. 2065–2074
[30] Yu, L., Chen, H., Dou, Q., *et al.*: 'Automated melanoma recognition in dermoscopy images via very deep residual networks', *IEEE Trans. Med. Imaging*, 2017, **36**, (4), pp. 994–1004
[31] Jafari, M.H., Karimi, N., Nasr-Esfahani, E., *et al.*: 'Skin lesion segmentation in clinical images using deep learning'. 23rd Int. Conf. on Pattern Recognition (ICPR), Cancun, Mexico, December 2016, pp. 337–342
[32] George, Y., Aldeen, M., Garnavi, R.: 'Skin hair removal for 2D psoriasis images'. 2015 Int. Conf. on Digital Image Computing: Techniques and Applications (DICTA), Adelaide, Australia, November 2015, pp. 1–8
[33] Maglogiannis, I., Delibasis, K.: 'Hair removal on dermoscopy images'. 2015 37th Annual Int. Conf. of the IEEE Engineering in Medicine and Biology Society (EMBC), Milan, Italy, August 2015, pp. 2960–2963
[34] Gutman, D., Codella, N.C.F., Celebi, E., *et al.*: 'Skin lesion analysis toward melanoma detection: a challenge at the International Symposium on Biomedical Imaging (ISBI) 2016, hosted by the International Skin Imaging Collaboration (ISIC)', CoRR, vol. abs/1605.01397, 2016
[35] Mendonca, T., Ferreira, P.M., Marques, J.S., *et al.*: 'Ph2 – a dermoscopic image database for research and benchmarking'. 2013 35th Annual Int. Conf. of the IEEE Engineering in Medicine and Biology Society (EMBC), Osaka, Japan, July 2013, pp. 5437–5440
[36] Pizer, S.M., Amburn, E.P., Austin, J.D., *et al.*: 'Adaptive histogram equalization and its variations', *Comput. Vision Graph. Image Process.*, 1987, **39**, (3), pp. 355–368
[37] Zuiderveld, K.: 'Graphics gems iv', in Heckbert, P.S. (Ed.): '*Contrast limited adaptive histogram equalization*' (Academic Press Professional, Inc., San Diego, CA, USA, 1994), pp. 474–485
[38] Frangi, A.F., Niessen, W.J., Vincken, K.L., *et al.*: '*Multiscale vessel enhancement filtering*' (Springer Berlin Heidelberg, Berlin, Heidelberg, 1998), pp. 130–137
[39] Telea, A.: 'An image inpainting technique based on the fast marching method', *J. Graph. Tools*, 2004, **9**, (1), pp. 23–34
[40] Boykov, Y.Y., Jolly, M.P.: 'Interactive graph cuts for optimal boundary & region segmentation of objects in n-d images'. Proc. Eighth IEEE Int. Conf. on Computer Vision, ICCV 2001, Vancouver, Canada, 2001, vol. 1, pp. 105–112
[41] Forgy, E.: 'Cluster analysis of multivariate data: efficiency versus interpretability of classification', *Biometrics*, 1965, **21**, (3), pp. 768–769
[42] Jancey, R.: 'Multidimensional group analysis', *Aust. J. Bot.*, 1966, **14**, (1), pp. 127–130
[43] Arthur, D., Vassilvitskii, S.: '*k*-means++: the advantages of careful seeding'. Proc. of the Eighteenth Annual ACM-SIAM Symp. on Discrete Algorithms, ser. SODA '07, Philadelphia, PA, USA, 2007, pp. 1027–1035